Two-photon entanglement in type-II parametric down-conversion

Y. H. Shih, A. V. Sergienko, and Morton H. Rubin
Department of Physics, University of Maryland Baltimore County, Baltimore, Maryland 21228

T. E. Kiess and C. O. Alley
Department of Physics, University of Maryland College Park, College Park, Maryland 20742
(Received 3 February 1994)

We present an experimental study of the entangled two-photon polarization states in type-II optical parametric down-conversion. It is interesting to see that the polarization entanglement depends on the detection spectral bandwidth, i.e., the bandwidth of the spectral filters placed in front of the detectors. The entanglement is also dependent on the length of the down-conversion crystal. A simple quantum model is provided to explain these phenomena.

PACS number(s): 03.65.Bz, 42.50.Wm

I. INTRODUCTION

Quantum-mechanical entanglement [1,2] has attracted a great deal of interest since the early days of quantum mechanics. An example of a two-particle entangled state was discussed in 1935 by Einstein, Podolsky, and Rosen such that the measurement of an observable of one particle determines the value of that observable for the other particle with unit probability [3,4]. Two-particle entangled states have been demonstrated in Einstein-Podolsky-Rosen (EPR)-type experiments and Bell's inequality measurements [5]. The two-photon entangled spin state in positronium annihilation was predicted by Wheeler and experimentally proved by Wu and Shaknov [6]. Atomic cascade decays were intensively used to produce similar two-photon entangled spin states to test Bell's inequalities [7,8]. Optical parametric down-conversion was introduced for the study of two-particle entanglement in the late 1980s and has recently attracted a great deal of attention [9].

In optical parametric down-conversion (OPDC), a pump beam is incident on a birefringent crystal. The pump beam is intense enough so that nonlinear effects lead to the spontaneous emission of a pair of light quanta highly correlated in phase space,

$$\omega_1+\omega_2=\omega_p,\quad \mathbf{k}_1+\mathbf{k}_2=\mathbf{k}_p\ , \tag{1}$$

where ω_i is the frequency and $\mathbf{k}_i$ the wave-number vector, linking pump (p), signal (1), and idler (2). The down-conversion is called type I or type II depending on whether the photons in the pair have parallel or orthogonal polarization. The pair of light quanta emerging from the nonlinear crystal may propagate in different directions or may propagate collinearly. The frequency and propagation directions are determined by the orientation of the nonlinear crystal, which reflects the phase-matching relations in Eq. (1). The type-I OPDC two-photon entanglement in spin or in space time has been demonstrated by different experiments in the past several years [10–17]. Two-particle spin entanglement for type-II OPDC was recently demonstrated in our laboratory under two experimental conditions: (1) detecting coincidences in narrow spectral bandwidth and (2) using a thin nonlinear crystal [18]. In contrast to type-I OPDC, the spin entanglement of the type-II OPDC light quanta pair depends on the detection bandwidth and the length of the nonlinear crystal. In this paper, we wish to report the experimental study of this detection bandwidth and crystal length dependent spin entanglement of type-II down-conversion. A simple quantum model is presented to explain this phenomenon.

Because the type-II OPDC photon pair is orthogonally polarized, we can easily produce a two-particle entangled state in linear, circular, and elliptical polarizations with the help of a quarter-wave plate and a beam splitter. The EPR-Bohm-type correlation and the corresponding Bell's inequality violation can be demonstrated in a simple beam-splitting experiment [18].

II. DETECTION BANDWIDTH DEPENDENCE OF THE ENTANGLED SPIN STATE

The experimental setup to study the effect of detection bandwidth and crystal length on the two-photon spin entanglement is illustrated in Fig. 1. A single-mode cw argon-ion laser line of 351.1 nm was used to pump a BBO (β-BaB_2O_4) nonlinear crystal. The BBO was cut for a type-II phase-matching angle to generate a pair of orthogonally polarized signal and idler photons degenerate in a 702.2-nm wavelength in a single beam. Two BBO crystals with lengths of 5.65 and 0.5 mm, respectively, were used in the experiments. The down-converted beam was separated from the pumping beam by a UV grade fused silica dispersion prism, then injected at a near normal incidence angle to a polarization independent beam splitter which has 50%-50% reflection and transmission coefficients. A detector package, which is composed of a Glan-Thompson linear polarization analyzer, a narrow bandwidth interference spectral filter, and a single photon detector, is placed in each transmission and reflection output port of the beam splitter. The photon detectors

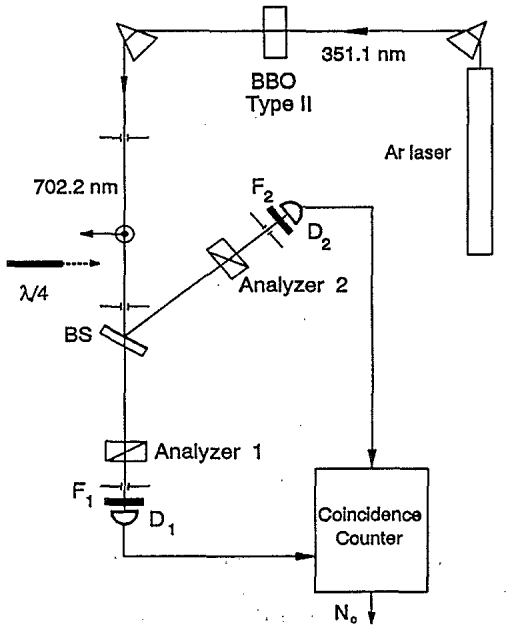

FIG. 1. Schematic diagram of the experiment. BS denotes a beam splitter, BBO is a β barium borate crystal, F is a filter and D is a photon detector.

are dry ice cooled avalanche photodiodes operated in the Geiger mode. The output pulses of the detectors are then sent to a coincidence circuit with a 3 nsec coincidence time window. The two detectors are separated by about 2 m, so that compared to the 3-nsec coincidence window, the detections are spacelike separated events.

The coincidence counting rates were studied as functions of angles θ_1 and θ_2, where θ_i is the angle between the axis of the ith polarization analyzer and the $\hat{\mathbf{x}}$ direction, which is defined by the o-ray polarization plane of the BBO crystal. Keep in mind that a right-handed natural coordinate system with respect to the $\mathbf{k}_i$ vector as the positive $\hat{\mathbf{z}}$ direction is employed for the discussions in this paper. The following form of coincidence rate as a function of θ_1 and θ_2 was observed in the experiments:

$$R_c = R_{c0}(\cos^2\theta_1\sin^2\theta_2+\sin^2\theta_1\cos^2\theta_2 - \rho\sin\theta_1\cos\theta_2\sin\theta_2\cos\theta_1) , \quad (2)$$

where ρ is a parameter that depends on the detection bandwidth, i.e., the bandwidth of the interference filters placed in front of the detector and the length of the BBO crystal. If $\rho=2$, Eq. (2) reduces to

$$R_c = R_{c0}\sin^2(\theta_1-\theta_2) , \quad (3)$$

which is the expected quantum correlation for the entangled two-photon polarization state,

$$|\Psi\rangle = (1/\sqrt{2})(|X_1\rangle\otimes|Y_2\rangle - |Y_1\rangle\otimes|X_2\rangle) . \quad (4)$$

$|\Psi\rangle$ quantum mechanically indicates a two-photon polarization state that is a superposition of the quantum states: (1) (o-ray transmitted) $\otimes$ (e-ray reflected) and (2) (e-ray transmitted) $\otimes$ (o-ray reflected) when the orthogonally polarized photon pair meets the beam splitter. On the other hand, if $\rho=0$ the interference cross term in Eq. (2) does not contribute, and we cannot detect the spin entanglement from the measurement.

Figure 2 reports the measured values of ρ for BBO crystals with lengths of 5.65- and 0.5 mm for different bandwidths of the filters. Note that for the 5.65-mm BBO crystal, ρ was always substantially less than 2 for the filters that were used in the measurements. For the 0.5-mm BBO, $\rho=1.98\pm0.04$ was achieved with a 1-nm bandwidth spectrum filter. The solid curves are the fits to a theoretical model which will be presented below. The values of ρ were obtained from the measurements of the coincidence rate as a function of θ_1 and θ_2. Figures 3 and 4 are typical measurements that reflect the different coincidence behavior for 5.65- and 0.5-mm BBO crystals. In Fig. 3, θ_1 was set to 45° and the coincidence rate was mapped out as a function of θ_2. In Fig. 4, both θ_1 and θ_2 were changed, keeping the sum of θ_1 and θ_2 equal to 90°. In both Figs. 3 and 4 the filters had 1-nm bandwidths. By fitting many similar curves, $\rho=0.72\pm0.07$ and $\rho=1.98\pm0.04$ were determined for 5.65- and 0.5-mm crystals, respectively, from these measurements.

For collinear type-II OPDC the two-photon part of the state that emerges from the down-conversion crystal may be calculated from the standard theory (first-order perturbation theory) to be [19,20]

$$|\Psi\rangle = \int d\omega_1\delta(\omega_1+\omega_2-\omega_p)\Psi(k_1+k_2-k_p) \times a_0^\dagger(\omega_1(k_1))a_e^\dagger(\omega_2(k_2))|0\rangle , \quad (5)$$

where ω and k represent the frequency and the wave number for signal (1), idler (2), and pump (p). The frequency phase-matching condition is explicitly displayed by the δ function; the wave-number phase-matching condition $\delta(k_1+k_2-k_p)$ is replaced by a sinc function $\psi(k_1+k_2-k_p)\equiv\psi(\Delta k)$, because of the finite length of the crystal [20]. The function $\psi(\Delta k)$ determines the natural spectral width of the two-photon state. The subscript indices o and e for the creation operators indicate the ordinary and extraordinary rays of the down-conversion, traveling along the same direction as the pump, the z direction. The coordinate axes x and y are chosen along the polarization direction of the o ray and the e ray, respectively. In this experiment we consider

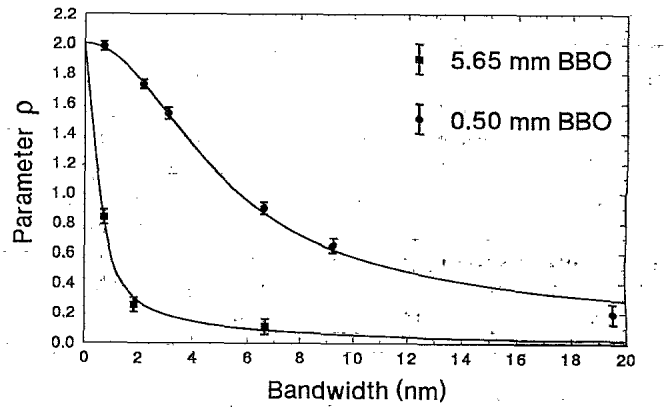

FIG. 2. Detection bandwidth and crystal length dependent entanglement.

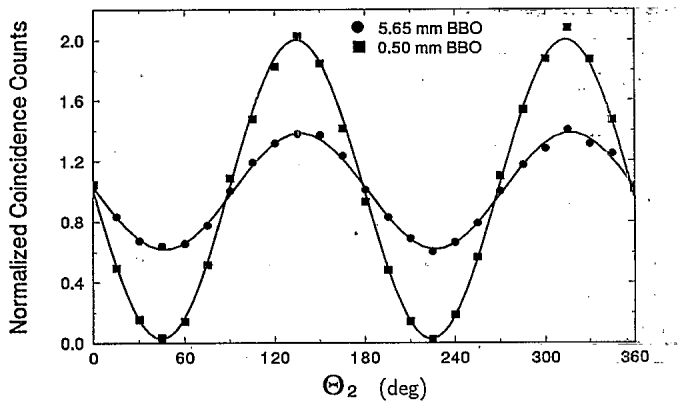

FIG. 3. Coincidence measurements for linear polarization states when θ_1 was set equal to 45°.

collinear down-conversion, and the use of small apertures makes state (5) a good one-dimensional approximation. The function $\psi(\Delta k)$ can be calculated from the standard theory of OPDC [20]. Taking the origin of the coordinates at the output surface of the down-conversion crystal,

$$\psi(\Delta k)=[1-\exp(-i\Delta kL)]/(i\Delta kL) , \tag{6}$$

where L is the length of the crystal. Suppose that the crystal is oriented so that the perfect phase-matching condition Eq. (1) is satisfied by a set Ω_o, Ω_e, k_o, and k_e (in this experiment we choose $\Omega_o=\Omega_e$). The finite bandwidth of the two-photon state, a result of the wave-number condition release, allows a frequency distribution such that $\omega_1=\Omega_o+\nu$ and $\omega_2=\Omega_e-\nu$, where $|\nu|\ll\Omega_{o,e}$. Now expand k_1 and k_2 to first order in ν using the dispersion relations

$$k_1=k_o+\nu(dk_o/d\Omega_o)=k_o-\nu/u_o ,$$

$$k_2=k_e-\nu(dk_e/d\Omega_e)=k_e-\nu/u_e ,$$

where u_o (u_e) is the group velocity for the ordinary (extraordinary) ray. Equation (6) can be written as

$$\psi(\nu)=[1-\exp(-i\nu DL)]/i\nu D , \tag{7}$$

where $D\equiv 1/u_o-1/u_e$.

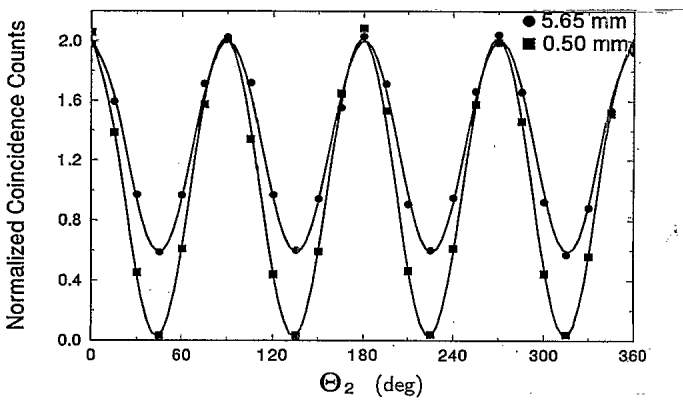

FIG. 4. Coincidence measurements for linear polarization states when $\theta_1+\theta_2=90°$ was preserved.

The fields at the detectors 1 and 2 are given by

$$\begin{aligned} E_1^{(+)}(t)&=\alpha_t\int d\omega f_1(\omega)\exp[-i\omega(t-\tau_1)] \\ &\quad\times\sum_j \hat{\mathbf{e}}_1\cdot\hat{\mathbf{e}}_j a_j(\omega) , \\ E_2^{(+)}(t)&=\alpha_r\int d\omega f_2(\omega)\exp[-i\omega(t-\tau_2)] \\ &\quad\times\sum_j \hat{\mathbf{e}}_2\cdot\hat{\mathbf{e}}_j a_j(\omega) , \end{aligned} \tag{8}$$

where a_j is the destruction operator of the photons, $j=o,e$, $\hat{\mathbf{e}}_i$ is in the direction of the ith linear polarization analyzer axis, $i=1,2$, and $\tau_i\equiv s_i/c$, where s_i is the optical path from the output surface of the BBO crystal to the ith detector, and c is the speed of light. α_t and α_r are the complex transmission and reflection coefficients of the beam splitter. The function $f_i(\omega)$, $i=1,2$, is the spectral transmission function of the filter in front of the ith detector. If we do not have the filters, $f(\omega)$ will be replaced by a constant. We will consider this case in the beginning of the following discussion.

The average coincidence counting rate is given by

$$\begin{aligned} R_c&=(1/T)\int\int_0^T dT_1dT_2\langle\Psi|E_1^{(-)}E_2^{(-)}E_2^{(+)}E_1^{(+)}|\Psi\rangle \\ &\quad\times S(T_1-T_2,\Delta T_c) \\ &=(1/T)\int\int_0^T dT_1dT_2|\Psi(t_1,t_2)|^2 S(T_1-T_2,\Delta T_c) , \end{aligned} \tag{9}$$

where $t_i\equiv T_i-\tau_i$, and T_i is the detection time of the ith detector. We assume $\tau_1=\tau_2$, i.e., equal distances from the output surface of the crystal to the detectors, to simplify the following discussion. T is the duration time of the measurement, $S(t,\Delta T_c)$ is a function that describes the coincidence circuit, ΔT_c is the time window of the coincidence circuit; for $|T_1-T_2|>\Delta T_c$, $S(t,\Delta T_c)\cong 0$, and for $|T_1-T_2|<\Delta T_c$, $S(t,\Delta T_c)\cong 1$. The counting time T may be taken to infinity as a good approximation, and if the coincidence time window is large enough we can set $S=1$ for all t.

An effective two-photon wave function $\Psi(t_1,t_2)$ is defined in Eq. (9),

$$\Psi(t_1,t_2)=\langle 0|E_1^{(+)}E_2^{(+)}|\Psi\rangle . \tag{10}$$

The introduction of $\Psi(t_1,t_2)$ is very helpful for understanding the physics. Suppose we do not use the spectral filters for the detectors; then the $f_i(\omega)$ function in Eq. (8) is replaced by a constant. Substituting (5) and (8) into (10), it is straightforward to show that

$$\begin{aligned} \Psi(t_1,t_2)&=\alpha_t\alpha_r v(t_1+t_2) \\ &\quad\times[\hat{\mathbf{e}}_1\cdot\hat{\mathbf{e}}_o\hat{\mathbf{e}}_2\cdot\hat{\mathbf{e}}_e u(t_1-t_2) \\ &\quad+\hat{\mathbf{e}}_i\cdot\hat{\mathbf{e}}_e\hat{\mathbf{e}}_2\cdot\hat{\mathbf{e}}_o u(-t_1+t_2)] , \end{aligned} \tag{11}$$

where

$$v(t)=v_0\exp(-i\omega_p t/2)\ , \tag{12}$$

$$u(t)=u_0\exp(-i\omega_d t/2)\times\int_{-\infty}^{\infty}d\nu[1-\exp(-\nu DL)]/(i\nu DL)\times\exp(-i\nu t)=\begin{cases}u_o\exp(-i\omega_d t/2), \\ DL>t>0 \\ 0 \quad \text{otherwise}\ ,\end{cases} \tag{13}$$

where v_0, u_0 are constants (normalization), and $\omega_d \equiv \Omega_o - \Omega_e$. We have approximated the pump to be a plane wave in the calculation. If the pump beam were taken to be a Gaussian with bandwidth σ_p, the constant v_0 would be replaced by a Gaussian function $v_0\exp(-\sigma_p^2 t^2/8)$. Because of the narrow spectral bandwidth of the pump beam, a plane wave is a good approximation for this experiment.

It is not difficult to understand the physics of the effective two-photon wave function (11). In the first term of the bracket the o ray goes to detector 1 and the e ray goes to detector 2; the function $u(t_1-t_2)$ means that whenever detector 2 is triggered detector 1 will be triggered at a later time, but no later than T_2+DL. In the second term the e ray goes to detector 1 and the o ray goes to detector 2; the function $u(-t_1+t_2)$ means that whenever detector 1 is triggered detector 2 will be triggered at a later time, but no later than T_1+DL. The "joint triggering" probability at T_1 and T_2 is a constant during these periods, and is zero otherwise. We may describe each of the terms as a two-dimensional wave packet in space time. The wave packets have an infinite large width along the axis of t_1+t_2 and a finite width of DL along the axis of t_1-t_2, however, the wave packet in the first term is centered at $DL/2$ and the wave packet in the second term is centered at $-DL/2$. These interpretations correspond to a reasonable physical picture for type-II OPDC. The photons are created in pairs, one with o polarization and the other with e polarization. If the pump is uniform, the pairs are created with equal probability at each point in the illuminated region of the crystal. BBO is a negative uniaxial crystal, so that the e ray exits the BBO crystal first. The maximum possible time delay between the o ray and the e ray is $(L/u_o - L/u_e)=DL$, which is the time delay to cross the crystal.

It is clear from Eqs. (11) and (13) that there is no interference because the two terms in the bracket are not overlapped in space time. Mathematically it is easy to see. Physically the o-ray and the e-ray photons are well distinguished in space time; it is impossible to find any detection time T_1 and T_2, except for $T_1=T_2$, in which the two terms in Eq. (11) both hold. If $T_1>T_2$ the detection only records the amplitude (o ray to D_1)$\otimes$(e ray to D_2); if $T_1<T_2$ the detection only records the amplitude (e ray to D_1)$\otimes$(o ray to D_2), and the chances of having the o-ray and e-ray photons exit from the BBO at $t_1=t_2$ (corresponds to $T_1=T_2$) is infinitesimal. It is obvious that $\rho=0$. The calculation of ρ is discussed below. In order to have interference the two terms in Eq. (11) must be overlapped in space time. It is very interesting to see that the spin entanglement can be achieved by placing narrow-bandwidth spectral filters in front of the detectors. The $f_i(\omega)$ function in Eq. (8) may be taken to be Gaussian,

$$f_i(\Omega_i-\omega)=f_0\exp[-(\Omega_i-\omega)^2/2\sigma^2]\ , \tag{14}$$

where we have assumed that the filters f_1 and f_2 are peaked around Ω_1 and Ω_2, respectively, with $\Omega_1+\Omega_2=\omega_p$. For simplicity we take them to have the same peak, shape, and bandwith σ. The function $u(t)$ is replaced by

$$u(t)=u_0\exp(-i\omega_d t/2)\int_{-\infty}^{\infty}d\nu f_1(\Omega_1+\nu)f_2(\Omega_2-\nu)[1-\exp(-\nu DL)]/(i\nu DL)\exp(-i\nu t)$$
$$=u_0\exp(-i\omega_d t/2)\{\mathrm{erf}(\sigma t/2)-\mathrm{erf}[(\sigma t-DL)/2]\}/2DL\ , \tag{15}$$

where $\mathrm{erf}(x)$ is the error function, and u_0 is a normalized constant. This function peaks at $DL/2$ and has a width on the order of $DL+8/\sigma$. It is clear now that the $u(t_1-t_2)$ and $u(-t_1+t_2)$ functions in Eq. (11) overlap; the narrower detection bandwidth and the shorter crystal length result in a larger overlap, so that a higher interference visibility leads to $p\Longrightarrow 2$. It is not difficult to understand the physics of this overlap based on the previous discussions.

It is straightforward to calculate the coincidence counting rate R_c from Eq. (9) by using the effective wave function (11). The result is shown in Eq. (2), and ρ is calculated as,

$$\rho=2\int_{-\infty}^{+\infty}dt\ \mathrm{Re}[u^*(t)u(-t)]\ . \tag{16}$$

The functions in (15) and (16) are easily evaluated numerically and fit the data with no free parameters. The solid lines in Fig. 2 are the theory curves for 5.65- an 0.5-mm BBO crystals. The curves agree with the measured values of ρ within reasonable experimental error. One can achieve $\rho\cong 2$ with a bandwidth less than 1 nm for a 0.5-mm BBO thin crystal.

III. TWO-PHOTON ENTANGLED STATES FOR LINEAR, CIRCULAR, AND ELLIPTICAL POLARIZATIONS

Using a 0.5-mm crystal and 1-nm bandwidth filters to achieve $\rho=2$, measurements for two-photon polarization entangled states were made. The use of a quarter-wave

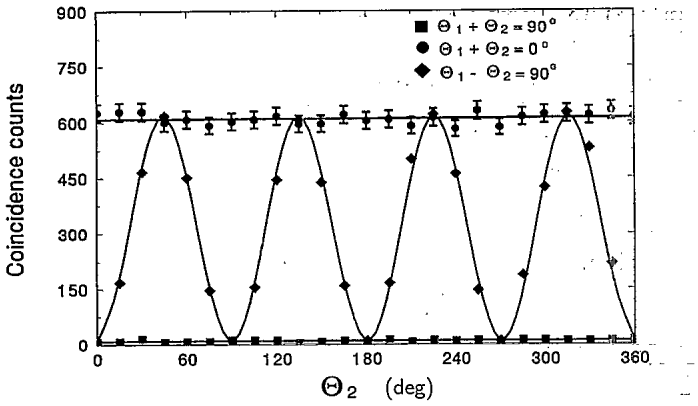

FIG. 5. Coincidence measurements for circular polarization Einstein-Podolsky-Rosen–Bohm state.

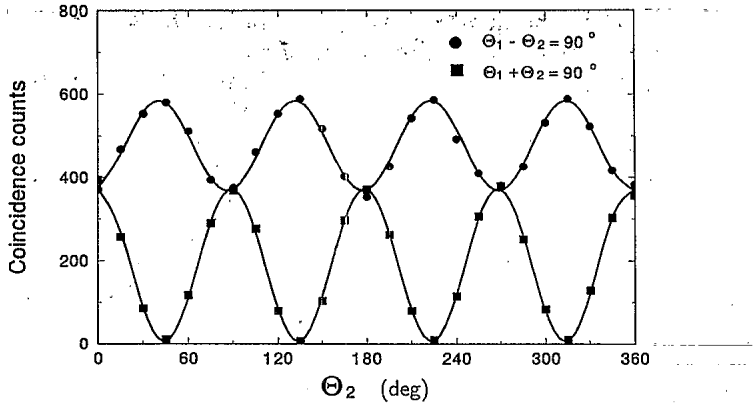

FIG. 7. Coincidence measurement for elliptical polarization state with quarter-wave plate oriented at 71.5°.

plate and a beam splitter can easily demonstrate the quantum-mechanical entanglement of arbitrary elliptical polarization states in type-II down-conversion. The experimental setup is the same as in Fig. 1, except a quarter-wave plate is placed after the 0.5-mm BBO crystal. If the fast axis of the quarter-wave plate is oriented at angle Φ with respect to the $\hat{\mathbf{x}}$ direction, the orthogonal linear polarization states $|X\rangle$ and $|Y\rangle$ are transformed to orthogonal elliptical polarization states:

$$\begin{aligned} |X\rangle &\Longrightarrow \cos(\Phi)|X'\rangle - i\sin(\Phi)|Y'\rangle \ , \\ |Y\rangle &\Longrightarrow \sin(\Phi)|X'\rangle + i\cos(\Phi)|Y'\rangle \ , \end{aligned} \tag{17}$$

where $|X'\rangle$ and $|Y'\rangle$ are in the direction of the fast and slow axes of the quarter-wave plate, respectively. After the beam splitter, a two-photon entangled state with elliptical polarizations is produced,

$$|\Psi\rangle = 1/\sqrt{2}\left[\begin{bmatrix}\cos(\Phi)\\ -i\sin(\Phi)\end{bmatrix}_1\begin{bmatrix}\sin(\Phi)\\ -i\cos(\Phi)\end{bmatrix}_2 + \begin{bmatrix}\sin(\Phi)\\ -i\cos(\Phi)\end{bmatrix}_1\begin{bmatrix}\cos(\Phi)\\ i\sin(\Phi)\end{bmatrix}_2\right] . \tag{18}$$

The coincidence counting rate for linear polarization analyzers is then,

$$R_c = R_{co}[\sin^2(2\Phi)\cos^2(\theta_1'+\theta_2') + \cos^2(2\Phi)\sin^2(\theta_1'-\theta_2')] \ , \tag{19}$$

where θ_i' is the angle between the axis of the ith polarization analyzer and the $|X_i'\rangle$ direction. Care has to be taken to follow the rules of natural coordinate system, especially for the reflected beam. Note that the direction of $|X_2'\rangle$ is opposite that of $|X_1'\rangle$.

If $\Phi=0°$, state (18) becomes state (4) which is a two-photon linear polarization entangled state. Quantum correlations given by Eq. (3) were observed experimentally [18]. Bell's inequality violation of 22 standard deviations was demonstrated [18].

For $\Phi=45°$, state (18) becomes the circular polarization EPR-Bohm state,

$$|\Psi\rangle = 1/\sqrt{2}(|R_i\rangle\otimes|R_2\rangle + |L_i\rangle\otimes|L_2\rangle) \ . \tag{20}$$

The expected quantum correlation

$$R_c = R_{c0}\cos^2(\theta_1+\theta_2) = R_{c0}\cos^2(\theta_1'+\theta_2') \tag{21}$$

was measured experimentally. Figure 5 reports the measured results. Note, in contrast to Eq. (3), here we have a function of $(\theta_1+\theta_2)$ instead of $(\theta_1-\theta_2)$. Circular polarization correlations in atomic cascade decay were demonstrated by Clauser [21].

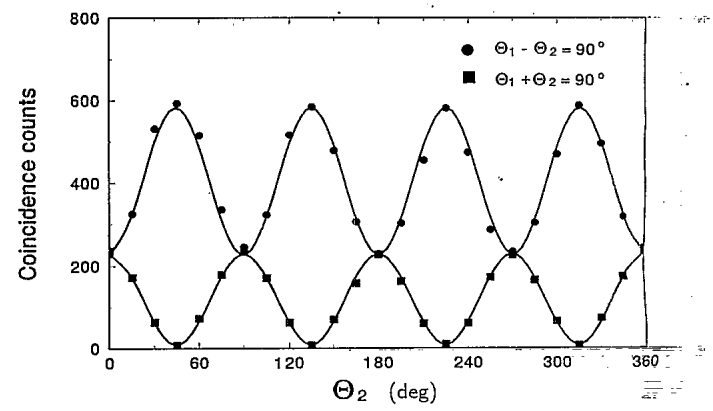

FIG. 6. Coincidence measurements for elliptical polarization state with quarter-wave plate oriented at 26.5°.

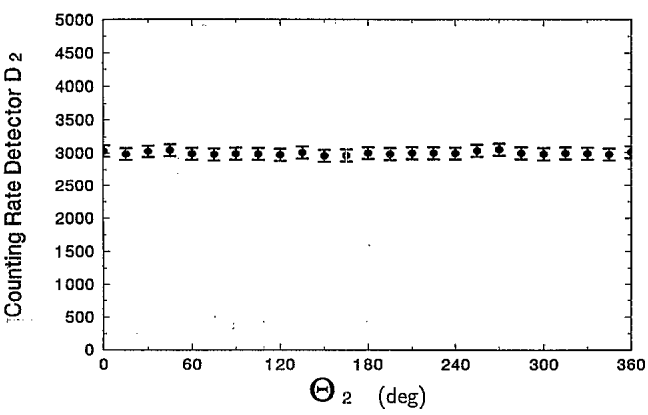

FIG. 8. Typical single detector counting rate.

When the quarter-wave plate was set to $\Phi=26.5°$ and 71.5°, respectively, Figs. 6 and 7 report four typical measurements that were taken under the conditions: $\theta_1'\pm\theta_2'=90°$. The solid lines in these figures are the theory curves of Eq. (19). The measured coincidence counting rates agree with Eq. (19) within reasonable experimental errors. Note, here, we use the θ' system to define the angles for the analyzers. Contrary to the coincidence counting rates, the single detector counting rates do not change with the θ angles for all the above measurements, as is reported in Fig. 8.

IV. CONCLUSION

In summary: A pair of orthogonally polarized light quanta is produced from type-II down-conversion in a single beam. The pair enters a single port of a beam splitter. There is no preferred polarization direction in each of the three beams (incident, transmitted, and reflected). However, if one of the photons, for example, the transmitted one, is detected to be linearly polarized in a certain direction, θ_1, the other one can be predicted with certainly to be linearly polarized in the direction θ_2, where θ_2 is not necessarily perpendicular to θ_1 The value of θ_2 depends on the quantum entangled state prepared by the observer. The measurement of the linear polarization (observable) for one particle determines the linear polarization (of that observable) for the other particle with unit probability. This is a typical two-particle entanglement discussed in the early days of quantum mechanics. In this paper we demonstrated the interesting phenomenon that the entangled polarization state in type-II OPDC depends on the detection bandwidth and the length of the OPDC crystal.

ACKNOWLEDGMENTS

We wish to thank D. N. Klyshko for helpful discussions, especially in understanding the theory of type-II parametric down-conversions. This work was supported partially by the Office of Naval Research Grant No. N00014-91-J-1430.

[1] E. Schrödinger, Naturwissenschaften **23**, 807, (1935); **23**, 823 (1935); **23**, 844 (1935). A translation of these papers appears in *Quantum Theory and Measurement,* edited by J. A. Wheeler and W. H. Zurek (Princeton University Press, Princeton, NJ, 1983).
[2] M. A. Horne, A. Shimony, and A. Zeilinger, Phys. Rev. Lett. **62**, 2209 (1989).
[3] A. Einstein, B. Podolsky, and N. Rosen, Phys. Rev. **47**, 777 (1935).
[4] D. Bohm, *Quantum Theory* (Prentice-Hall, Englewood Cliffs, NJ, 1951).
[5] J. S. Bell, Physics **1**, 195 (1964).
[6] C. S. Wu and I. Shaknov, Phys. Rev. **77**, 136 (1950).
[7] For a review, see J. F. Clauser and A. Shimony, Rep. Prog. Phys. **41**, 1881 (1976).
[8] A. Aspect, P. Grangier, and G. Roger, Phys. Rev. Lett. **47**, 460 (1981); **49**, 91 (1982); A. Aspect, J. Dalibard, and G. Roger, *ibid.* **49**, 1804 (1982).
[9] D. M. Greenberger, M. Horne, and A. Zeilinger, Phys. Today **46** (8), 23 (1993).
[10] Y. H. Shih and C. O. Alley, Phys. Rev. Lett. **61**, 2921 (1988).
[11] Z. Y. Ou and L. Mandel, Phys. Rev. Lett. **61**, 50 (1988).
[12] C. K. Hong, Z. Y. Ou, and L. Mandel, Phys. Rev. Lett. **59**, 2044 (1987).
[13] Z. Y. Ou and L. Mandel, Phys. Rev. Lett. **61**, 54 (1988).
[14] J. G. Rarity and P. R. Tapster, Phys. Rev. Lett. **64**, 2495 (1990).
[15] J. Brendel, E. Mohler, and W. Martienssen, Phys. Rev. Lett. **66**, 1142 (1991).
[16] P. G. Kwiat, A. M. Steinberg, and R. Y. Chiao, Phys. Rev. A **47**, 2472 (1993).
[17] T. S. Larchuk, R. A. Campos, J. G. Rarity, P. R. Tapster, E. Jakeman, B. E. A. Saleh, and M. C. Teich, Phys. Rev. Lett. **70**, 1603 (1993).
[18] T. E. Kiess, Y. H. Shih, A. V. Sergienko, and C. O. Alley, Phys. Rev. Lett. **71**, 3893 (1993).
[19] W. H. Louisell, A. Yariv, and A. E. Siegman, Phys. Rev. **124** 1646 (1961).
[20] D. N. Klyshko, *Photons and Nonlinear Optics* (Gordon and Breach, New York, 1988).
[21] J. F. Clauser, Nuovo Cimento **33**, 740 (1976).